

Research Article



Cyclic fatigue resistance of M-Pro and RaCe Ni-Ti rotary endodontic instruments in artificial curved canals: a comparative *in vitro* study

Hadeer Mostafa El Feky , Khalid Mohammed Ezzat ,
Marwa Mahmoud Ali Bedier

Department of Endodontics, Faculty of Dentistry, Cairo University, Cairo, Egypt



Received: Jul 10, 2019

Revised: Sep 18, 2019

Accepted: Sep 24, 2019

El Feky HM, Ezzat KM, Bedier MM

*Correspondence to

Marwa Mahmoud Ali Bedier, BDS, MSc, MD

Associate Professor, Department of
Endodontics, Faculty of Dentistry, Cairo
University, 12 El Saraya Street, Manial ElRoda,
Cairo 11451, Egypt.

E-mail: m.bedier81@gmail.com

Copyright © 2019. The Korean Academy of
Conservative Dentistry

This is an Open Access article distributed
under the terms of the Creative Commons
Attribution Non-Commercial License ([https://
creativecommons.org/licenses/by-nc/4.0/](https://creativecommons.org/licenses/by-nc/4.0/))
which permits unrestricted non-commercial
use, distribution, and reproduction in any
medium, provided the original work is properly
cited.

Conflict of Interest

No potential conflict of interest relevant to this
article was reported.

Author Contributions

Conceptualization: El Feky HM, Ezzat KM,
Bedier MM; Data curation: El Feky HM, Ezzat
KM, Bedier MM; Formal analysis: El Feky HM,
Ezzat KM, Bedier MM; Funding acquisition:
El Feky HM; Investigation: El Feky HM, Ezzat
KM, Bedier MM; Methodology: El Feky HM;
Project administration: El Feky HM, Bedier MM;
Resources: El Feky HM; Software: El Feky HM,
Ezzat KM, Bedier MM; Supervision: Ezzat KM,
Bedier MM; Validation: El Feky HM, Bedier MM;

ABSTRACT

Objectives: To compare the flexural cyclic fatigue resistance and the length of the fractured segments (FLs) of recently introduced M-Pro rotary files with that of RaCe rotary files in curved canals and to evaluate the fracture surface by scanning electron microscopy (SEM).

Materials and Methods: Thirty-six endodontic files with the same tip size and taper (size 25, 0.06 taper) were used. The samples were classified into 2 groups (n = 18): the M-Pro group (M-Pro IMD) and the RaCe group (FKG). A custom-made simulated canal model was fabricated to evaluate the total number of cycles to failure and the FL. SEM was used to examine the fracture surfaces of the fragmented segments. The data were statistically analyzed and comparisons between the 2 groups for normally distributed numerical variables were carried out using the independent Student's *t*-test. A *p* value less than 0.05 was considered to indicate statistical significance.

Results: The M-Pro group showed significantly higher resistance to flexural cyclic fatigue than the RaCe group ($p < 0.05$), but there was no significant difference in the FLs between the 2 groups ($p \geq 0.05$).

Conclusions: Thermal treatment of nickel-titanium instruments can improve the flexural cyclic fatigue resistance of rotary endodontic files, and the M-Pro rotary system seems to be a promising rotary endodontic file.

Keywords: Canals; Flexural resistance; Fracture; Instruments; Microscopy




INTRODUCTION

Adequate cleaning and shaping of the root canal system is essential for successful endodontic therapy. Most instrumentation techniques in which stainless steel instruments are used in curved canals pose the risk of zipping, ledge formation, and apical transportation; therefore, new generations of endodontic instruments have been developed using nickel-titanium (NiTi) alloys, which potentially allow the shaping of narrow and curved root canals without any aberrations [1,2].

Austenitic NiTi instruments are characterized by their super-elastic behavior, due to the reversible phase transformation between the austenitic and martensitic phases of the alloy

Visualization: Ezzat KM; Writing - original draft: El Feky HM, Ezzat KM, Bedier MM; Writing - review & editing: El Feky HM, Bedier MM.

ORCID iDs

Hadeer Mostafa El Feky 
<https://orcid.org/0000-0002-8728-9024>
Khalid Mohammed Ezzat 
<https://orcid.org/0000-0001-7322-9023>
Marwa Mahmoud Ali Bedier 
<https://orcid.org/0000-0001-8214-0602>

when stress is induced in the structure in response to load application. The shape memory effect is caused by the ability of deformed NiTi instruments to recover their original shape due to the phase transformation of the deformed martensite to the stable austenite phase by heating. The presence of the stable martensite phase within the microstructure of NiTi instruments makes them more flexible and more resistant to cyclic fatigue fracture [3].

Despite the advantageous properties of NiTi instruments, they are not free from sudden unexpected file separation during clinical use. Fractures may occur through either torsional or flexural cyclic fatigue [4]. Flexural cyclic fatigue has an unpredictable clinical incidence; it occurs suddenly after free rotation of a certain number of cycles in a curved root canal as the file is being compressed (compressive stress) on the inner curved surface and elongated (tensile stress) on the outer curve. This bending and unbending of the file may cause surface crack formation at these regions of tensile stress concentration, resulting in breakage [5,6]. Several attempts have been made to enhance the fatigue resistance of NiTi instruments by improving the cross-sectional design, the manufacturing process, or the surface treatment, as well as by introducing new alloys [7,8].

The RaCe rotary endodontic system (FKG, La Chaux De Fonds, Switzerland) has been developed from an austenite NiTi alloy. It is characterized by a triangular cross-section, with 2 short, sharp alternating cutting edges that are placed at a different angle along the file length due to the alternating twisting and untwisting segments, thereby reducing the screw-in effect; furthermore, electrochemical polishing enhances its resistance to fatigue and corrosion [9,10]

Recently, the M-Pro rotary endodontic system (M-Pro IMD, Guangdong, China) was introduced. This system is made from a specially treated X-wire that has pre-bending ability, greater flexibility, and higher resistance to cyclic fatigue, with a convex triangle cross-section, an increasing pitch of the cutting edges, and less of a screwing effect. The manufacturer claims that it has high fracture resistance and can remain centralized in the canal [11].

Within the scope of the present research, no study has yet compared the cyclic fatigue resistance of the M-Pro rotary endodontic system and RaCe rotary endodontic system. Therefore, the main objective of the present study was to fill this knowledge gap. The null hypothesis was that there would be no significant difference between the M-Pro rotary endodontic file and the RaCe rotary endodontic file regarding cyclic fatigue resistance in a curved canal.

MATERIALS AND METHODS

Sample size calculation

The sample size calculation was based on the results of AlShwaimi [12] utilizing the number of the cycles to fracture as the outcome. Using an alpha (α) level of 0.05 (5%) and a beta (β) level of 0.20 (20%) (*i.e.*, power = 80% at a 5% significance level) and a difference between the 2 groups of 50 ± 51.3 , the minimum estimated sample size was 18 samples per group. The sample size calculation was performed using PS (Power and Sample Size Calculation software version 3.1.2, Vanderbilt University, Nashville, TN, USA).

Classification of the samples

Thirty-six rotary endodontic NiTi files were used, and the samples were divided into 2 groups ($n = 18$) according the type of instrument used. In the M-Pro group, M-Pro rotary files (size

25 and 6% taper) were rotated in a custom-made simulated canal model with a 60° angle of curvature and a 5 mm radius of curvature, while in the RaCe group, RaCe rotary files (size 25 and 6% taper) were rotated in the same model.

All files were inspected for any manufacturing defects using a stereomicroscope, and none were discarded.

Evaluation of flexural cyclic fatigue

1. Fabrication of the custom-made simulated canal model

A custom made-simulated canal model was fabricated from hardened stainless steel to be able to withstand friction wear, with a 60° angle of curvature, 5 mm radius of curvature, 2 mm depth, and 16 mm length (11 mm straight portion and 5 mm curved portion). The model was machined according to the recommendations of Pruett *et al.* [13], and the canal measurements were manipulated using AUTOCAD software (Autodesk, San Rafael, CA, USA). The drawing was estimated from the size and tapers of the tested instruments; however, the canal was wider than the file by 0.2 mm along its length to reduce friction and allow the file to rotate freely (diameter at D0 mm = 0.45 mm; diameter at D16 mm = 1.41 mm). A transparent glass top cover was fixed to the model to observe the file while rotating it until fracture and to prevent its slippage during rotation. At the apical end, there was a circular reservoir to collect the fractured pieces of the instruments.

2. Cyclic fatigue testing

A computer-controlled material testing machine (Model LRX-plus, Lloyd instruments Ltd., Fareham, UK) composed of an upper movable compartment and a lower fixed base was used for cyclic fatigue testing. The contra-angled hand piece (NSK 20:1 contra-angled hand piece, Nakanishi Inc., Tochigi, Japan) of an endodontic electric-torque-controlled-speed reduction motor (NSK Endo-Mate Dt, Nakanishi Inc.) was locked in a reproducible position by a custom-made jig. This jig was then attached to an adapter that screwed into the upper movable compartment, while the custom-made simulated canal model was secured to the lower fixed compartment of the testing machine by tightening the screws.

A synthetic lubricant oil was applied to the simulated canal until it was fully flooded with oil before each test. Moreover, the rotary files were painted with the lubricant before use to reduce the friction between the rotary files and the stainless-steel canal model to avoid generating heat. Each of the tested files was attached to the contra-angle hand piece and then was inserted into the middle of the simulated canal perpendicular to the orifice at the exact depth with the help of the rubber stopper (**Figure 1**). All files were allowed to rotate freely

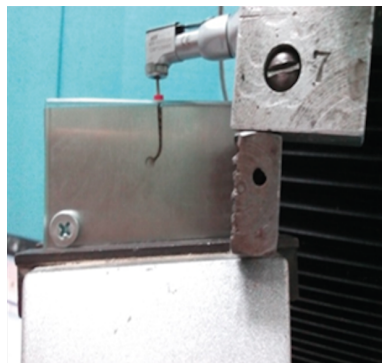


Figure 1. File attached to the contra-angled hand piece and inserted within the simulated canal, fixed to the lower compartment of the testing machine.

within the simulated canal according to the manufacturer's instructions (speed of 500 rpm and torque of 1.5 N•cm) at room temperature, until fracture.

Instrument fracture was detected both visually by observation through the transparent glass and automatically by the computer software, and the time was recorded in seconds from the beginning of rotation until the moment of fracture. The total number of cycles to failure (NCF) was calculated by multiplying the time to fracture in minutes by the number of rotations per minute (500 rpm).

$$\text{NCF} = \text{Time to fracture in minutes} \times \text{Number of rotations per minute}$$

3. Fractured segment measurement

For each file, the length of the fractured segment (FL) was measured using a precision digital caliper (Pinrui, Digital LCD Caliper, Shanghai, China) with a resolution of 0.01 mm.

4. Examination of the fractured files using scanning electron microscopy (SEM)

The separated files were ultrasonically cleaned in 70% ethyl alcohol for 15 minutes before examination under SEM (SEM Model Quanta 250 FEG [Field Emission Gun], FEI Company, Eindhoven, The Netherlands) to remove any remnants of the lubricating oil and the debris entrapped between the flutes or in the fracture surface during flexural cyclic fatigue testing, and then allowed to dry. Two representative samples from each file system were randomly selected and photographed using SEM at magnifications of $\times 400$ and $\times 1,500$ for the cross-sectional views and $\times 300$ and $\times 600$ for the lateral views to verify the fracture mode.

5. Statistical methods

Numerical data were explored for normality by checking the distribution of data and using tests of normality (Kolmogorov-Smirnov and Shapiro-Wilk tests). All data showed a normal (parametric) distribution. Parametric data are presented as mean and standard deviation (SD). Comparisons between the 2 groups for normally distributed numerical variables were made using the independent Student's *t*-test. The significance level was set at $p \leq 0.05$. Statistical analysis was performed with SPSS version 20 for Windows (IBM Corp., Armonk, NY, USA).

RESULTS

The mean and SD of the NCF and FL values of the 2 tested groups are summarized in **Table 1**.

A statistically significant difference was found between the 2 groups ($p = 0.05$), with the M-Pro group showing a higher NCF than the RaCe group. However, there was no statistically significant difference in the mean FL between both groups ($p = 0.488$).

Table 1. The mean, standard deviation (SD), range, and results of the independent Student's *t*-test comparing the number of cycles to failure (NCF) and the fractured segment length (FL) between the 2 tested groups (M-Pro and RaCe)

Variable	M-Pro (n = 18)		RaCe (n = 18)		p value
	Mean \pm SD	Range	Mean \pm SD	Range	
NCF	3,380.6 \pm 1,221.7	1,170–6,605	404.1 \pm 127.0	250–585	0.05*
FL (mm)	3.4 \pm 0.9	1.2–4.6	3.2 \pm 0.5	2.4–4.3	0.488

*Indicates significance at $p \leq 0.05$.

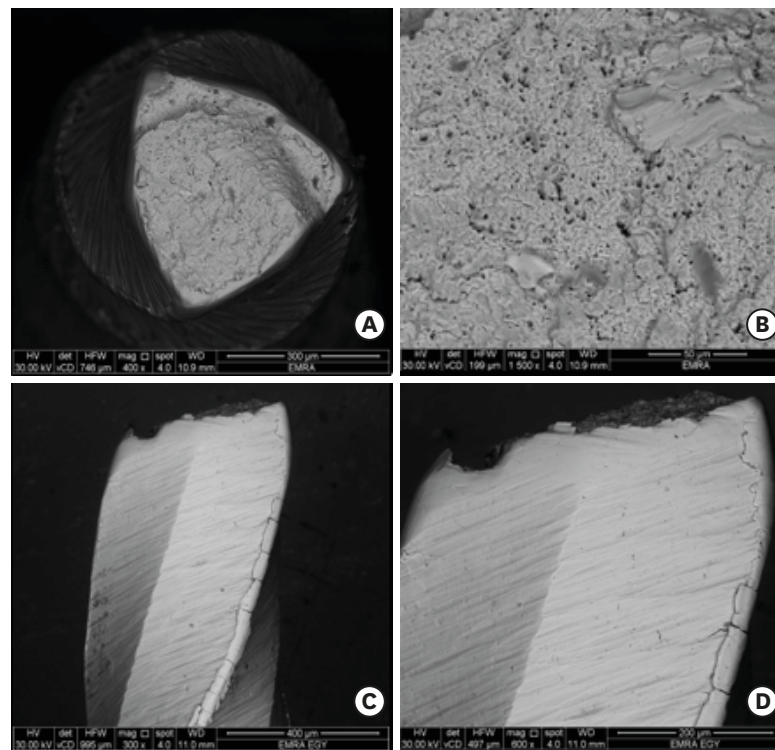


Figure 2. (A) A scanning electron micrograph of the fractured surface (cross-sectional view) of a representative sample of the M-Pro group after cyclic fatigue testing using low magnification ($\times 400$) shows the general features of cyclic fatigue failure such as fatigue zones followed by an overload zone (fast fracture) with numerous dimples, microvoids, fatigue striations, and fracture lines extending on different planes, indicating multiple crack origins, in addition to crack propagation at the smooth area. (B) Using high magnification ($\times 1,500$), the surface details were clearer, including irregular morphology, an extensive rough dimpled surface, microporosities, microvoids, fatigue striations, and multiple microcracks. (C) A scanning electron micrograph of the lateral surface of a representative sample of the M-Pro group using low magnification ($\times 300$) shows multiple cracks and surface irregularities. (D) Using higher magnification ($\times 600$), extensive cracks can be seen.

The surface of the FLs of the samples from each group was photographed under SEM, and revealed characteristic patterns of fatigue fractures, including crack initiation at the cutting edges of the fracture cross-sections. The areas of crack initiation and growth exhibited small regions of nucleation, known as smooth regions, peripheral to the cross-section. Slow fatigue crack propagation is characterized by striations. The fractures started from the periphery of the instrument, and moved towards the center. The presence of microvoids, crater-like formations, and dimpling (associated with ductile fracture) was observed (**Figures 2 and 3**).

DISCUSSION

The fracture of endodontic instruments during root canal preparation is of major concern because it can make root canal treatment more difficult. Many factors can affect the risk of instrument fracture inside the root canal, such as the abruptness of the canal curvature, including the angle, radius, and position of the maximum curvature center, as well as the instrument alloy, design, surface treatment, rotational speed, kinematics, and the operator's skill [14,15].

Currently, there is no specification or international standard for testing the cyclic fatigue resistance of endodontic rotary instruments. As a consequence, several devices and methods

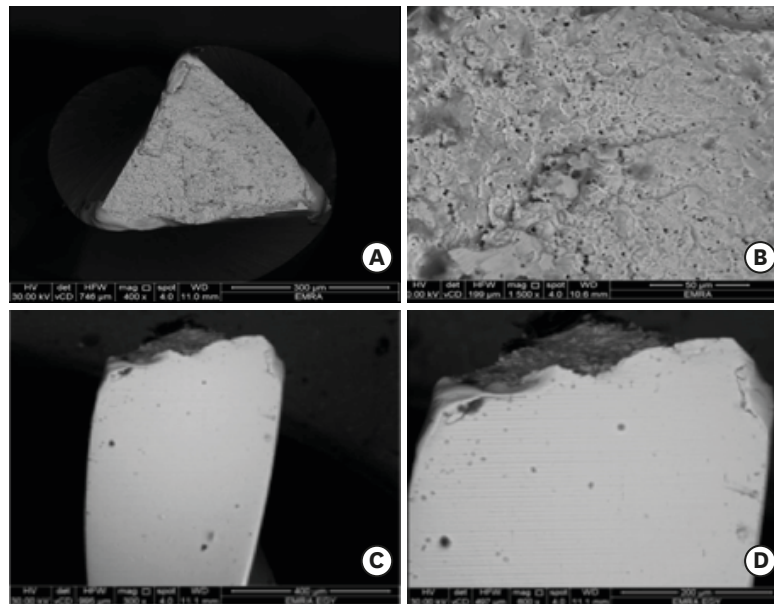


Figure 3. (A) A scanning electron micrograph of the fractured surface (cross-sectional view) of a representative sample of the RaCe group after cyclic fatigue testing using low magnification ($\times 400$) shows the general features of cyclic fatigue failure, such as fatigue zones followed by an overload zone (fast fracture), with numerous dimples and microvoids. (B) Using higher magnification ($\times 1,500$), microvoids can be seen beside the dimples, but to a lesser extent than in the M-Pro group. (C) A scanning electron micrograph of the lateral surface of a representative sample of the RaCe group using low magnification ($\times 300$) shows a smooth surface with no sign of plastic deformation. (D) Using a higher magnification ($\times 600$), a smooth surface can be seen with a small number of microcracks.

have been used to investigate the *in vitro* flexural cyclic fatigue fracture resistance of NiTi rotary endodontic instruments. In nearly all studies reported in the endodontic literature, the rotating instrument was either confined in a glass or metal tube, in a grooved block-and-rod assembly, or in a sloped metal block [13,16,17].

Although using natural human teeth would be the ideal method to evaluate the flexural cyclic fatigue resistance of endodontic instruments, as they can accurately simulate clinical conditions, a limitation of such tests is that a tooth can only be used once because the shape of the root canal changes during instrumentation, making it impossible to standardize the experimental conditions [16]. Therefore, in the present study, a custom-made stainless steel canal model was used to ensure a fixed radius of curvature, a fixed angle of curvature, and a fixed center of maximum curvature [13].

Cyclic fatigue resistance was tested at room temperature [18,19], as the conventional super-elastic NiTi instrument has an austenite structure at room temperature, while those manufactured from controlled memory wire using a proprietary thermomechanical technique have a mixture of martensite and austenite at room temperature. The presence of more martensite at the expense of austenite makes the files extremely flexible, but without the shape memory of other NiTi files, in addition to increasing the cyclic fatigue resistance [20].

The design of the simulated canal used in the study followed the method described by Pruett *et al.* [13]. This method describes the root canal curvature based on the angle of curvature and the radius of curvature. The radius of curvature represents how abruptly or severely a specific angle of curvature occurs as the canal deviates from a straight line. The smaller the radius of

curvature, the more abrupt the canal deviation, and the stress on the instrument is inversely related to the radius of canal curvature [13]. The cyclic fatigue life span of endodontic instruments decreases as the angle of curvature increases, the radius of curvature decreases, and the rotational speed and instrument diameter increase; therefore, the metal mass of the instrument at the point of maximum stress is another important factor [13,21].

In the present study, all the previously mentioned factors were fixed and standardized, except for the method of the instruments' manufacturing and design. The simulated canal had a 60° angle of curvature, a 5 mm radius of curvature, and a point of maximum curvature that was at 5 mm from the apex of the canal to simulate the apical curvature that can be found clinically, where the maximum stresses on the instrument are concentrated, as has been done in previous studies [12,22,23]. These values also reflect the findings of Pruett *et al.* [13], who reported that low stress levels were induced by curvature less than 30° and at a radius of 5 mm. Thus in an attempt to simulate a more acute curvature, the present study used a 60° angle of curvature and a 5 mm radius of curvature, thereby simulating abrupt apical curvature patterns that can be found clinically and facilitating comparisons with other studies.

The artificial canal reproduced the instrument's size and taper, thereby providing the instrument with a suitable trajectory to ensure the accuracy of the canal size, as done in previous studies [12,22]. An extra space of 0.2 mm was added along the canal length in accordance with Plotino *et al.* [24], who studied the influence of 3 designs of artificial canals on the trajectory of the tested file and reported that artificial canals with a tapered shape and larger dimensions (tip size and taper) than the original dimensions of the instrument by 0.1 mm had the best design for representing the parameters of the selected curvature, while the second best option was increasing the size by 0.3 mm. In the present study, only an increase by 0.2 mm was feasible due to technical limitations. Nonetheless this allowed the file to rotate freely in the canal, avoiding any torsional stresses that may develop as a result of locking during rotation.

In the results of the present study, M-Pro rotary endodontic files constructed from specially treated X-wire with pre-bending ability showed a higher NCF than RaCe rotary endodontic files constructed from a conventional NiTi alloy. These results are in agreement with those reported by Shen *et al.* [20], Chang *et al.* [22], Çapar *et al.* [25], Çapar *et al.* [26], Pedullà *et al.* [27], Topçuoğlu *et al.* [28], Amato *et al.* [29], AlShwaimi [12], and Karataşlıoğlu *et al.* [30], who reported that instruments manufactured from controlled memory wire with thermomechanical treatment showed higher resistance to flexural cyclic fatigue than other conventional instruments. In addition, Yao *et al.* [5] reported that K3 files (size 25/0.04) were significantly more resistant to failure than ProFiles and RaCe files.

These results may be attributed to the type of the wire and the proprietary heat treatment used to manufacture M-Pro instruments, in which thermomechanical treatment improves the crystal structure arrangement and the mechanical properties. Increasing the stable martensite phase enhances resistance to fatigue-crack growth and flexibility when compared to conventional NiTi [3,31].

RaCe rotary endodontic files are constructed from a conventional NiTi alloy, which mainly consists of the austenite phase during clinical use as the austenite finishing temperature for most conventional NiTi files is at or below room temperature, whereas the austenite finishing temperature of controlled memory files is markedly above body temperature (about 50°C).

This austenite phase is harder and less flexible than the martensite phase, with less resistance to flexural cyclic fatigue [32].

The design of RaCe rotary endodontic files also plays an important role in cyclic fatigue resistance [4]. The alternating cutting edges in the RaCe rotary file design constantly switch the helix angles of the blades as they rotate inside the canal, thereby preventing the file from engaging excessively in the canal walls; this design acts to concentrate stress at specific points, rather than distributing it along the entire file length [33].

The results of the present study showed that there was no difference in the FLs between M-Pro rotary endodontic files and RaCe rotary endodontic files, in agreement with Plotino *et al.* [34] Çapar *et al.* [26], Pedullà *et al.* [27], Topçuoğlu *et al.* [28], and Karataşlıoğlu *et al.* [30].

In the present study, the FL ranged from 1.2 to 4.6 mm in the M-Pro group and from 2.4 to 4.3 mm in the RaCe group. This lower range in the M-Pro group may have been due to its flexibility, which makes it assume a different trajectory within the same canal curvature, as the stiffness of each instrument—based on its design—can cause it to follow a specific trajectory within the same curvature, because instruments have different bending properties [24]. Instruments subjected to flexural cyclic fatigue were fractured near the center of the curvature as a result of the concentration of maximum stresses at the most curved part of the canal [34].

Fractography can be defined broadly as the science of observing, measuring, and interpreting a fractured surface topography. When material failure occurs involving actual breakage, fractography can be used to identify the origin of the fracture, the direction of crack propagation, the failure mechanism, the nature of the stresses, and material defects. Fractographic analysis is an integral part of cyclic fatigue testing, as it reveals the history of the fractured interfaces [35,36].

Fracture mechanics theory always assumes the existence of a flaw or crack in the solid mass, which is capable of growing or propagating to cause failure. The crack propagates when the stress reaches a critical value that can overcome the force of cohesion [37].

In the present study, SEM analysis revealed that all instruments showed a peripheral small smooth fatigue zone with the origins of microcracks and clusters of striations at the periphery, followed by an overload zone that was characterized by the presence of dimples and microvoids, which are characteristic of ductile fracture that occurs through the coalescence of microvoids [37].

It is recommended that further research should investigate the effect of temperature on the cyclic fatigue resistance of instruments manufactured from conventional NiTi alloys and those that receive thermomechanical treatment, in addition to the effects of different canal curvatures, locations of curvature, and number of clinical uses on cyclic fatigue resistance.

CONCLUSIONS

Thermal treatment of NiTi instruments can improve their flexural cyclic fatigue resistance, as M-Pro rotary endodontic files showed a higher NCF than RaCe rotary endodontic files when

used in a custom-made simulated canal model. There was no significant difference in the FL between the 2 groups, and SEM examinations of the fracture surfaces showed multiple cracks, fatigue striations, a dimpled surface, and voids, which indicate a ductile mode of fracture.

REFERENCES

1. Saunders Elizabeth M. Hand instrumentation in root canal preparation. *Endod Topics* 2005;10:163-167.
[CROSSREF](#)
2. Stavileci M, Hoxha V, Görduysus Ö, Tatar I, Laperre K, Hostens J, Küçükkaya S, Muhaxheri E. Evaluation of root canal preparation using rotary system and hand instruments assessed by micro-computed tomography. *Med Sci Monit Basic Res* 2015;21:123-130.
[PUBMED](#)
3. Zupanc J, Vahdat-Pajouh N, Schäfer E. New thermomechanically treated NiTi alloys - a review. *Int Endod J* 2018;51:1088-1103.
[PUBMED](#) | [CROSSREF](#)
4. Parashos P, Messer HH. Rotary NiTi instrument fracture and its consequences. *J Endod* 2006;32:1031-1043.
[PUBMED](#) | [CROSSREF](#)
5. Yao JH, Schwartz SA, Beeson TJ. Cyclic fatigue of three types of rotary nickel-titanium files in a dynamic model. *J Endod* 2006;32:55-57.
[PUBMED](#) | [CROSSREF](#)
6. Martín B, Zelada G, Varela P, Bahillo JG, Magán F, Ahn S, Rodríguez C. Factors influencing the fracture of nickel-titanium rotary instruments. *Int Endod J* 2003;36:262-266.
[PUBMED](#) | [CROSSREF](#)
7. Gao Y, Gutmann JL, Wilkinson K, Maxwell R, Ammon D. Evaluation of the impact of raw materials on the fatigue and mechanical properties of ProFile Vortex rotary instruments. *J Endod* 2012;38:398-401.
[PUBMED](#) | [CROSSREF](#)
8. Gambarini G, Rubini AG, Al Sudani D, Gergi R, Culla A, De Angelis F, Di Carlo S, Pompa G, Osta N, Testarelli L. Influence of different angles of reciprocation on the cyclic fatigue of nickel-titanium endodontic instruments. *J Endod* 2012;38:1408-1411.
[PUBMED](#) | [CROSSREF](#)
9. Tripi TR, Bonaccorso A, Condorelli GG. Cyclic fatigue of different nickel-titanium endodontic rotary instruments. *Oral Surg Oral Med Oral Pathol Oral Radiol Endod* 2006;102:e106-e114.
[PUBMED](#) | [CROSSREF](#)
10. Azimi S, Delvari P, Hajarian HC, Saghiri MA, Karamifar K, Lotfi M. Cyclic fatigue resistance and fractographic analysis of RaCe and Protaper rotary NiTi instruments. *Iran Endod J* 2011;6:80-86.
[PUBMED](#)
11. Seeddent Co., Ltd.: M-Pro rotary endodontic system. Available from: <http://seeddent-com.sell.everychina.com/p-107759691-dental-mpro-files.html> (updated 2019 Nov 5).
12. AlShwaimi E. Cyclic fatigue resistance of a novel rotary file manufactured using controlled memory Ni-Ti technology compared to a file made from M-wire file. *Int Endod J* 2018;51:112-117.
[PUBMED](#) | [CROSSREF](#)
13. Pruett JP, Clement DJ, Carnes DL Jr. Cyclic fatigue testing of nickel-titanium endodontic instruments. *J Endod* 1997;23:77-85.
[PUBMED](#) | [CROSSREF](#)
14. Parashos P, Gordon I, Messer HH. Factors influencing defects of rotary nickel-titanium endodontic instruments after clinical use. *J Endod* 2004;30:722-725.
[PUBMED](#) | [CROSSREF](#)
15. Shen Y, Cheung GS, Peng B, Haapasalo M. Defects in nickel-titanium instruments after clinical use. Part 2: fractographic analysis of fractured surface in a cohort study. *J Endod* 2009;35:133-136.
[PUBMED](#) | [CROSSREF](#)
16. Yared GM, Bou Dagher FE, Machtou P. Cyclic fatigue of Profile rotary instruments after simulated clinical use. *Int Endod J* 1999;32:115-119.
[PUBMED](#) | [CROSSREF](#)
17. Plotino G, Grande NM, Cordaro M, Testarelli L, Gambarini G. A review of cyclic fatigue testing of nickel-titanium rotary instruments. *J Endod* 2009;35:1469-1476.
[PUBMED](#) | [CROSSREF](#)

18. Elnaghy AM. Cyclic fatigue resistance of ProTaper Next nickel-titanium rotary files. *Int Endod J* 2014;47:1034-1039.
[PUBMED](#) | [CROSSREF](#)
19. Plotino G, Grande NM, Cotti E, Testarelli L, Gambarini G. Blue treatment enhances cyclic fatigue resistance of vortex nickel-titanium rotary files. *J Endod* 2014;40:1451-1453.
[PUBMED](#) | [CROSSREF](#)
20. Shen Y, Qian W, Abtin H, Gao Y, Haapasalo M. Fatigue testing of controlled memory wire nickel-titanium rotary instruments. *J Endod* 2011;37:997-1001.
[PUBMED](#) | [CROSSREF](#)
21. Turpin YL, Chagneau F, Vulcain JM. Impact of two theoretical cross-sections on torsional and bending stresses of nickel-titanium root canal instrument models. *J Endod* 2000;26:414-417.
[PUBMED](#) | [CROSSREF](#)
22. Chang SW, Shim KS, Kim YC, Jee KK, Zhu Q, Perinpanayagam H, Kum KY. Cyclic fatigue resistance, torsional resistance, and metallurgical characteristics of V taper 2 and V taper 2H rotary NiTi files. *Scanning* 2016;38:564-570.
[PUBMED](#) | [CROSSREF](#)
23. Pedullà E, Plotino G, Grande NM, Pappalardo A, Rapisarda E. Cyclic fatigue resistance of four nickel-titanium rotary instruments: a comparative study. *Ann Stomatol (Roma)* 2012;3:59-63.
[PUBMED](#)
24. Plotino G, Grand NM, Mazza C, Petrovic R, Testarelli L, Gambarini G. Influence of size and taper of artificial canals on the trajectory of NiTi rotary instruments in cyclic fatigue studies. *Oral Surg Oral Med Oral Pathol Oral Radiol Endod* 2010;109:e60-e66.
[PUBMED](#) | [CROSSREF](#)
25. Çapar ID, Ertas H, Arslan H. Comparison of cyclic fatigue resistance of novel nickel-titanium rotary instruments. *Aust Endod J* 2015;41:24-28.
[PUBMED](#) | [CROSSREF](#)
26. Çapar ID, Kaval ME, Ertas H, Sen BH. Comparison of the cyclic fatigue resistance of 5 different rotary pathfinding instruments made of conventional nickel-titanium wire, M-wire, and controlled memory wire. *J Endod* 2015;41:535-538.
[PUBMED](#) | [CROSSREF](#)
27. Pedullà E, Lo Savio F, Boninelli S, Plotino G, Grande NM, La Rosa G, Rapisarda E. Torsional and cyclic fatigue resistance of a new nickel titanium instrument manufactured by electrical discharge machining. *J Endod* 2016;42:156-159.
[PUBMED](#) | [CROSSREF](#)
28. Topçuoğlu HS, Topçuoğlu G, Akti A, Düzgün S. *In vitro* comparison of cyclic fatigue resistance of ProTaper Next, HyFlex CM, OneShape, and ProTaper Universal instruments in a canal with a double curvature. *J Endod* 2016;42:969-971.
[PUBMED](#) | [CROSSREF](#)
29. Amato M, Pantaleo G, Abdellatif D, Blasi A, LoGiudice R, Iandolo A. Evaluation of cyclic fatigue resistance of modern nickel-titanium rotary instruments with continuous rotation. *G Ital Endod* 2017;31:78-82.
30. Karataşlıoğlu E, Aydın U, Yıldırım C. Cyclic fatigue resistance of novel rotary files manufactured from different thermal treated nickel-titanium wires in artificial canals. *Niger J Clin Pract* 2018;21:231-235.
[PUBMED](#)
31. Shen Y, Zhou HM, Zheng YF, Peng B, Haapasalo M. Current challenges and concepts of the thermomechanical treatment of nickel-titanium instruments. *J Endod* 2013;39:163-172.
[PUBMED](#) | [CROSSREF](#)
32. Srivastava S, Alghadouni MA, Alotheem HS. Current strategies in metallurgical advances of 450 rotary NiTi instruments: a review. *J Dent Health Oral Disord Ther* 2018;9:00333.
[CROSSREF](#)
33. Subramaniam V, Indira R, Srinivasan MR, Shankar P. Stress distribution in rotary nickel titanium instruments - a finite element analysis. *J Conserv Dent* 2007;10:112-118.
[CROSSREF](#)
34. Plotino G, Grande NM, Sorci E, Malagnino VA, Somma F. A comparison of cyclic fatigue between used and new Mtwo Ni-Ti rotary instruments. *Int Endod J* 2006;39:716-723.
[PUBMED](#) | [CROSSREF](#)
35. Oh SR, Chang SW, Lee Y, Gu Y, Son WJ, Lee W, Baek SH, Bae KS, Choi GW, Lim SM, Kum KY. A comparison of nickel-titanium rotary instruments manufactured using different methods and cross-sectional areas: ability to resist cyclic fatigue. *Oral Surg Oral Med Oral Pathol Oral Radiol Endod* 2010;109:622-628.
[PUBMED](#) | [CROSSREF](#)

36. Grande NM, Plotino G, Pecci R, Bedini R, Malagnino VA, Somma F. Cyclic fatigue resistance and three-dimensional analysis of instruments from two nickel-titanium rotary systems. *Int Endod J* 2006;39:755-763.
[PUBMED](#) | [CROSSREF](#)
37. Cheung GS, Darvell BW. Fatigue testing of a NiTi rotary instrument. Part 2: fractographic analysis. *Int Endod J* 2007;40:619-625.
[PUBMED](#) | [CROSSREF](#)